European Journal of Medicinal Chemistry 84 (2014) 708–717

Contents lists available at ScienceDirect

European Journal of Medicinal Chemistry

journal homepage: http://www.elsevier.com/locate/ejmech

Original article

Synthesis and evaluation of the cytotoxic activity of 1,2-furanonaphthoquinones tethered to 1,2,3-1*H*-triazoles in myeloid and lymphoid leukemia cell lines

Mariana F.C. Cardoso [b, 1], Patrícia C. Rodrigues [a, 1], Maria Eduarda I.M. Oliveira [a], Ivson L. Gama [b], Illana M.C.B. da Silva [b], Isabela O. Santos [b], David R. Rocha [b], Rosa T. Pinho [c], Vitor F. Ferreira [b], Maria Cecília B.V. de Souza [b], Fernando de C. da Silva [b, *], Floriano Paes Silva-Jr [a, *]

[a] Fundação Oswaldo Cruz, Instituto Oswaldo Cruz, Laboratório de Bioquímica de Proteínas e Peptídeos, 21040-360, Rio de Janeiro, RJ, Brazil
[b] Universidade Federal Fluminense, Instituto de Química, Departamento de Química Orgânica, Campus do Valonguinho, 24210-141, Niterói, RJ, Brazil
[c] Fundação Oswaldo Cruz, Instituto Oswaldo Cruz, Laboratório de Imunologia Clínica, 21040-360, Rio de Janeiro, RJ, Brazil

ARTICLE INFO

Article history:
Received 18 May 2014
Received in revised form
20 July 2014
Accepted 22 July 2014
Available online 23 July 2014

Keywords:
Naphthoquinone
1,2,3-Triazole
Organic synthesis
Cytotoxic activity
Leukemia
Cancer

ABSTRACT

Leukemia is the most common blood cancer, and its development starts at diverse points, leading to distinct subtypes that respond differently to therapy. This heterogeneity is rarely taken into account in therapies, so it is still essential to look for new specific drugs for leukemia subtypes or even for therapy-resistant cases. Naphthoquinones (NQ) are considered privileged structures in medicinal chemistry due to their plethora of biological activities, including antimicrobial and anticancer effects. Nitrogen-containing heterocycles such as 1,2,3-1*H*-triazoles have been identified as general scaffolds for generating glycosidase inhibitors. In the present study, the NQ and 1,2,3-1*H*-triazole cores have been combined to chemically synthesize 18 new 1,2-furanonaphthoquinones tethered to 1,2,3-1*H*-triazoles (1,2-FNQT). Their cytotoxicities were evaluated against four different leukemia cell lines, including MOLT-4 and CEM (lymphoid cell lines) and K562 and KG1 (myeloid cell lines), as well as normal human peripheral blood mononucleated cells (PBMCs). The new 1,2-FNQT series showed high cytotoxic potential against all leukemia cell lines tested, and some compounds (**12o** and **12p**) showed even better results than the classical therapeutic compounds such as doxorubicin or cisplatin. Others compounds, such as **12b**, are promising because of their high selectivity against lymphoblastic leukemia and their low activity against normal hematopoietic cells. The cells of lymphoid origin (MOLT and CEM) were generally more sensitive than the myeloid cell lines to this series of compounds, and most of the compounds that showed the highest cytotoxicity were similarly active against both cell lines.

1. Introduction

Acute leukemia is one of the most aggressive hematopoietic malignancies and is characterized by the abnormal proliferation of the immature cells of the hematopoietic system. As a set of very heterogeneous diseases, acute leukemia is commonly divided into Acute Lymphoblastic Leukemia (ALL) and Acute Myeloid Leukemia (AML) depending on the precursor cell. Both forms are clonal hematopoietic stem cell malignancies thought to follow a "Two Hit" model of disease origin [1], in which at least two genetic mutations are necessary to trigger the expansion of a clonal population of cells that is blocked from differentiating into mature cells. The leukemic clone may arise at different stages of differentiation of the lymphoid and myeloid precursors, which results in the development of multiple subtypes of leukemia that can be characterized by distinct biochemical and morphological aspects [2,3].

ALL is the most common type of cancer in children and also has diverse subtypes. Whereas ALL prognosis and survival have shown a large improvement over the last forty years, reaching 70%–80% [4,5], children with AML experience a worse prognosis, with overall survival rates of only 40%–60% under intensive chemotherapy [6–8]. Furthermore, the complete remission rate differs, with 5%–

* Corresponding authors.
E-mail addresses: gqofernando@vm.uff.br (F.C. da Silva), floriano@ioc.fiocruz.br (F.P. Silva-Jr).
[1] These authors contributed equally to this work.

http://dx.doi.org/10.1016/j.ejmech.2014.07.079
0223-5234/

10% induction failures in AML resulting from refractory disease and toxicity as opposed to only 1%–2% induction failures in ALL.

Despite these advances in survival rates during the several decades, the expected 5-year survival rate for all patients diagnosed with AML in the United States is a dismal 21% while ALL has a 5-year survival rate of 65% [9]. Survival becomes even worse in patients over 50 years of age, in which case the 5-year survival is 11% (AML) and 16% (ALL) [10]. The drug resistance mechanisms causing treatment failure remains a challenge in the fight against leukemia, especially for several AML subtypes or for patients who either do not achieve remission or relapse. Moreover, resistance is observed not only with conventional chemotherapy but also with targeted therapies, i.e., the so-called "smart drugs", such as kinase inhibitors and tamoxifen, which binds to the estrogen receptor [11].

Each patient harbors a different cancer with respect to which genes are mutated, the nature of each mutation (i.e., different mutations for the same gene have been detected in several patients) [12], and the order of appearance of these mutations. Furthermore, tumors are very heterogeneous due to the clonal evolution of tumor cell populations driven by genomic instability [13]. These observations partly explain why different patients harboring the "same" cancer may respond differently to the same treatment regimen.

Quinones have diverse biological activities [14] and some are in use or under clinical trials for cancer treatment. These include the natural products daunorubicin (**1**) and doxorubicin (**2**); streptonigrin (**3**) and mytomicin C (**4**) (*N*-heterocyclic quinones) (Fig. 1); and lapachol (**5**) [15] (Fig. 2). Several studies have shown that quinones owe their activity against cancer cells either to inhibition of the nuclear enzymes topoisomerases I and II [16,17] or to the generation of reactive oxygen species (ROS), ultimately inducing DNA damage that is followed by cell apoptosis [18–20]. The anti-tumor specificity of quinones is generally due to overexpression of topoisomerases and the associated deficiency of protection mechanisms against DNA damage in cancer cells, or to the increase in topoisomerase bioactivation by the NAD(P)H:quinone oxidoreductase 1 (NQO1), which is an abundant enzyme in many tumors [21].

Fig. 2 shows a group of natural (**5**, **6**) and synthetic (**7**–**10**) naphthoquinones, of which lapachol (**5**) and β-lapachone (**6**) [22] are the best known members [23,24] due to several biological activities that include anti-tumor effects [25]. Nor-lapachol (**7**) is a synthetic derivative that can be obtained either by a degradation reaction with H_2O_2, called Hooker degradation [26,27], or by condensation of 2-hydroxy-1,4-naphthoquinone (Lawsone) with isobutyraldehyde [28].

Nor-lapachol can be cyclized under acid catalysis to yield nor-β-lapachone (**8**), which has selective cytotoxicity to human lymphocytes and HL-60 leukemia cells and murine fibroblasts V79 [29]. This 1,4-naphthoquinone can also be reacted with bromine in the presence of nucleophiles to substitute nor-β-lapachone at the dihydrofuran ring. Several 3-arylamino-nor-β-lapachone derivatives were synthesized by this route and were found to be highly potent against some cancer cells including HL60, with IC_{50} below 2 μM (**9a**–**c**) [30,31]. Other synthetic furanonaphthoquinones (FNQ) obtained by effective one-pot cascade reactions of 3-phenyliodonio-1,2,4-trioxo-1,2,3,4-tetrahydronaphthalenides with 3-butyn-2-ol showed moderate cytotoxicity against human leukemia U937 and HL-60 cells with IC_{50} below 4.9 μM [32].

The 1,2,3-1*H*-triazole nucleus is a remarkably important pharmacophore group in medicinal chemistry [33,34] because it has been incorporated into several compounds that present important biological activities. Novel and improved anticancer agents have recently been designed by molecular hybridization of known cytotoxic compounds with 1,2,3-1*H*-triazol [35]. Five 1,2,3-1*H*-triazoles coupled to β-lapachone have been synthesized and assayed against some cancer cell lines [36], and compounds **10a** and **10b** were found to be the most active against HL-60 leukemia.

The diversity of responses to therapy and the need to improve therapies against certain subtypes of AML, acute leukemia in older people, and even disease relapse, prompted us to look for more specific and safer drugs that could efficiently personalize therapy or improve patient survival in standard protocols against leukemia. In view of the promising results achieved with 1,2-furanonaphthoquinones tethered to 1,2,3-1*H*-triazole (1,2-FNQT) on the HL-60 cell line, we synthesized an extended series of such hybrid compounds. In investigating the cytotoxicity and specificity of these compounds, we considered cell origin and used four different leukemia cell lines: CCRF-CEM and MOLT-4 (lymphoid origin); and K562 and KG1 (myeloid origin). Furthermore, we evaluated the selectivity for leukemia over normal hematopoietic cells by assaying the compounds on peripheral blood mononuclear cells obtained from normal human donors.

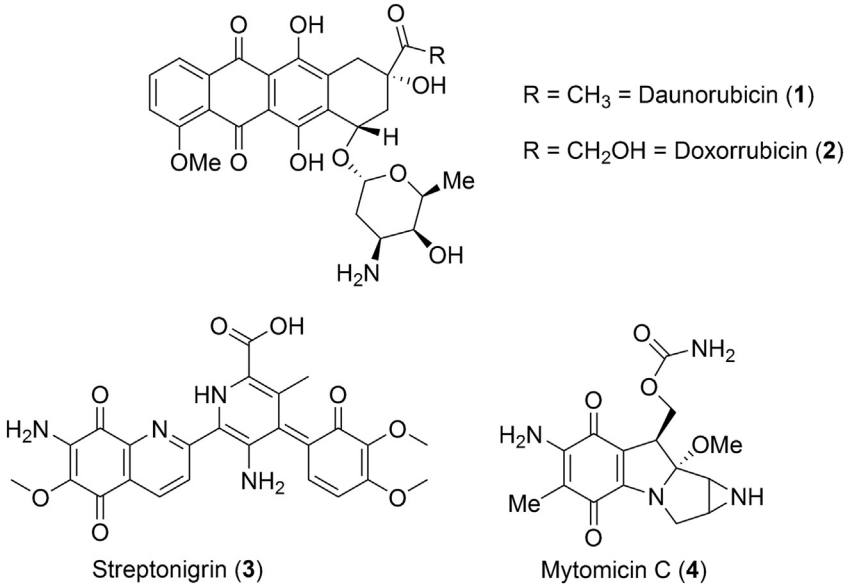

Fig. 1. Examples of quinones that are in clinical use or trials for cancer treatment.

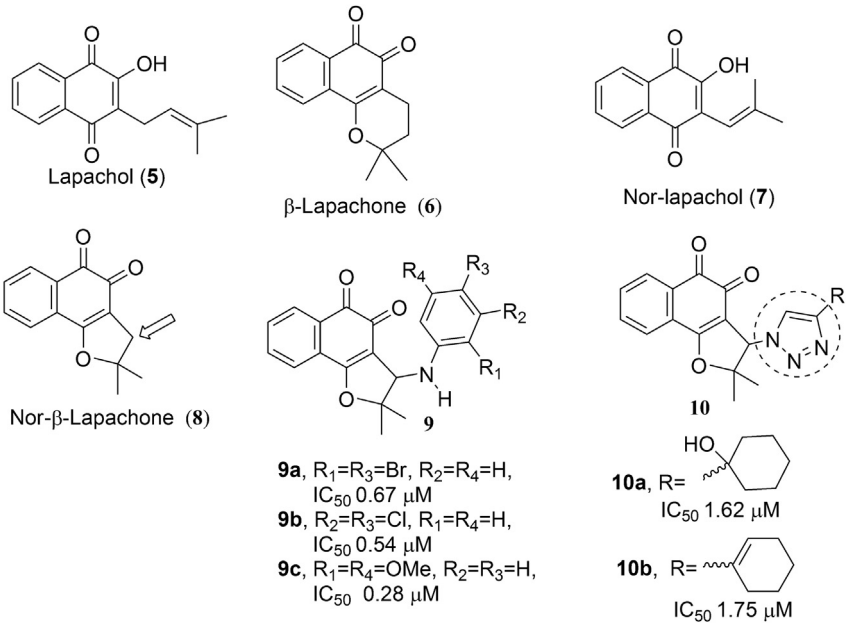

Fig. 2. Some bioactive synthetic and natural naphthoquinones. Shown IC_{50} values are for HL60 cells (see Ref. [30] for (**9a**–**c**) and Ref. [36] for **10a**,**b**).

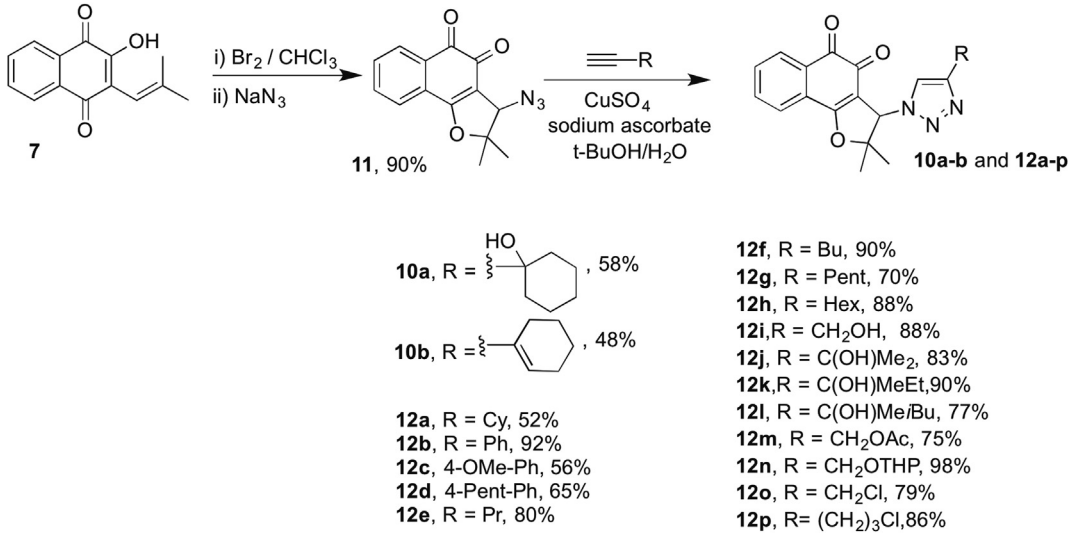

Fig. 3. General scheme used for preparation of 1,2-furanaphthoquinone triazoles **10a**,**b** and **12a**–**p**.

Finally, we used simple computational models to predict the drug-like characteristics and infer the predicted physicochemical and toxicological properties of 1,2-FNQTs to determine their potential as new anti-leukemia drugs.

2. Results and discussion

2.1. Chemistry

All 2,2-dimethyl-3-(4-(alkyl or aryl)-1*H*-1,2,3-triazol-1-yl)-2,3-dihydronaphtho[1,2-*b*]furan-4,5-dione were prepared by known synthetic routes [36]. The methodology was based on the Huisgen 1,3-dipolar cycloaddition reaction between the key intermediate **11** (3-azido-2,2-dimethyl-2,3-dihydro-naphtho[1,2-b]furan-4,5-dione) and the appropriate terminal alkynes, which were catalyzed by Cu(I) and provided only the 1,4-regioisomers (Fig. 3). Most compounds were obtained in high yields (>75%).

2.2. Hemolytic activity

Hemolysis was assayed to evaluate possible adverse effects induced by surfactant compounds, which could lead to cellular membrane damage and therefore unspecific cytotoxicity. All compounds were evaluated at a concentration of 1000 μM (Fig. 4). In cases where hemolysis was higher than 5% at 1000 μM, the compound was re-tested at 200 μM (e.g., for compounds **12d** and **12o**).

Of the compounds tested, only **12d** and **12o** presented any significant hemolysis (>5%) at 1000 μM. After re-testing **12d** and **12o** at 200 μM, neither showed significant hemolysis (data not shown). Thus, the concentration of 200 μM was utilized as the maximum concentration in cytotoxicity assays with Alamar Blue®.

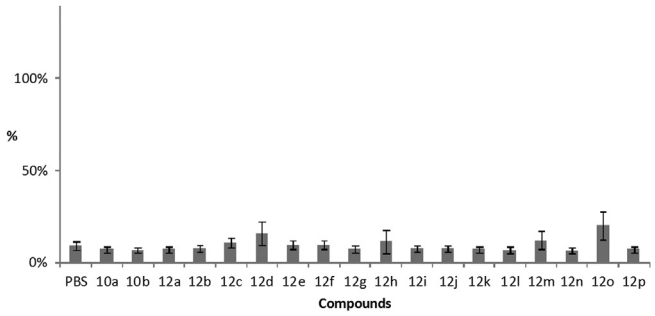

Fig. 4. Hemolytic activity of the 1,2,3-1*H*-triazol derivatives of nor-β-lapachone at 1000 μM. Osmotic shock with milli-Q H_2O (100% hemolysis) was used as a positive control and PBS was added as a negative control.

Table 1
Standardized conditions for the cytotoxic assay with AlamarBlue®.

Cell/cell line	Cells/well	Incubation time with AlamarBlue®
CCRF-CEM	2.5×10^4	2 h
MOLT-4	2.5×10^4	6 h
K562	2.5×10^4	4 h
KG1	5.0×10^4	6 h
Normal PBMC	5.0×10^4	24 h

2.3. Cytotoxicity in leukemia cell lines

All compounds were characterized for their cytotoxic effects on the four leukemia cell lines by their cell viability inhibition (IC_{50}) values and the results are summarized in Table 2. Potencies for IC_{50} were directly determined without performing a preliminary screening step at a fixed compound concentration due to the known cytotoxic effects of the nor-β-lapachone moiety present on these hybrid molecules.

Our results showed that all compounds were cytotoxic to the four cell lines with different potencies (IC_{50} values ranging from 0.05 to 83.44 μM). Many compounds within this new series of 1,2-FNQTs showed an improved cytotoxic potential with the four cell lines tested when compared with the precursor nor-β-lapachone. Overall, the hybrid compounds were more active than nor-β-lapachone against the lymphoid cell lines MOLT and CEM but showed less of a pronounced improvement in cytotoxicity for the K562 cell line.

The most potent compounds (**12p**, **12m**, **12o**, **12b** and **12i**) were the same for the MOLT and CEM lymphoid cell lines, while compound **12c** had low cytotoxicity in both cell lines.

Among the compounds showing submicromolar IC_{50} values, we identified the following: **10b** on MOLT (0.28 μM); **12b** on MOLT

Table 2
Cytotoxic activity on 48 h incubation of the nor-β-lapachone tethered triazoles with the four leukemia cell lines MOLT, CEM, KG1 and K562.

Compounds		MOLT		CEM		KG1		K562	
		IC_{50} (μM)	SD	IC_{50} (μM)	SD	IC_{50} (μM)	SD	IC_{50} (μM)	SD
Nor-β-Lapachone		13.6	0.4	15.2	2.1	17.2	1.6	2.28	0.11
11 (azide deriv.)		3.64	0.24	3.18	0.36	6.06	0.67	1.58	0.36
Cisplatin		nt	–	nt	–	113	37	304	88
Doxorubicin		0.07	0.02	0.15	0.02	nt	–	nt	–
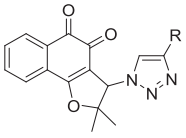									
	R								
10a		2.58	0.32	2.79	0.18	4.92	0.15	1.53	0.29
10b		0.28	0.22	12.6	0.9	8.41	0.86	1.11	3.75
12a		2.13	0.22	1.97	0.82	7.62	0.76	3.80	0.41
12b		0.75	0.15	1.96	0.19	12.8	1.5	14.4	3.9
12c	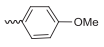	34.5	1.8	11.7	1.9	76.2	7.1	9.06	0.82
12d	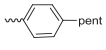	2.62	0.31	13.8	1.5	3.92	0.44	8.03	0.81
12e	Pr	1.47	0.22	3.14	0.81	1.55	0.42	60.9	10.4
12f	Bu	1.92	0.39	3.73	0.06	3.79	0.23	3.78	0.33
12g	Pentyl	2.28	0.25	27.6	2.0	30.0	3.6	2.68	0.42
12h	Hexyl	2.17	0.69	7.30	7.53	5.58	0.39	–	–
12i	CH_2OH	1.35	2.78	1.53	0.58	5.33	0.19	1.58	0.47
12j	$C(Me)_2OH$	2.16	0.42	1.73	0.96	2.00	1.57	2.43	0.15
12k	COH(Et)(Me)	1.98	0.58	3.57	0.13	5.63	0.48	1.39	0.25
12l	C(iBu)(Me)OH	1.47	0.59	1.77	0.05	1.32	0.06	1.91	0.05
12m	CH_2OAc	0.16	0.01	0.31	0.06	9.58	0.98	8.35	0.20
12n	CH_2OTHP	2.04	0.28	3.16	0.14	5.63	2.53	1.84	0.33
12o	CH_2Cl	0.48	0.02	0.67	0.03	12.27	4.89	1.38	0.13
12p	$(CH_2)_3Cl$	0.05	0.03	0.34	0.01	11.07	0.93	2.07	0.23

Cisplatin and Doxorubicin were used as standard anticancer compounds. The precursor compounds and intermediates, nor-lapachol and nor-β-lapachone and its azide derivative, were assayed for comparative purposes. Cytotoxicity, expressed by IC_{50}, was measured by the Alamar Blue method. nt = not tested.

(0.75 μM); **12m** on MOLT (0.16 μM), CEM (0.31 μM) and KG1 (0.98 μM); **12o** on MOLT (0.48 μM) and CEM (0.67 μM); and **12p** on MOLT (0.05 μM), CEM (0.34 μM) and KG1 (0.93 μM). With the exception of **10b**, the anticancer activities of all compounds are reported here for the first time.

Although the activity data are complex due to intrinsic differences for each cell line and multiple factors affecting the observed cytotoxicity (e.g., cell permeability Vs macromolecular target binding), some trends in SAR (structure–activity relationship) could still be derived. By comparing the IC_{50} values of the derivatives bearing a cyclic R group substituting C-4 of the 1,2,3-1*H*-triazol ring on the MOLT cell line, we observed that all these bulk substituents except 4-OMe phenyl contributed to the improved potency of the derivatives over the parent nor-β-lapachone. Among the hybrid triazoles carrying aliphatic hydroxylated R groups in C-4 (**12i**–**l**), the effects of the alkyl chain length or branching were negligible, with IC_{50} values ranging from 1.35 to 2.16 μM. On the other hand, acetylation of the hydroxyl of **12i** resulted in compound **12m**, which was 5 to 10-times more active on lymphoid cell lines MOLT and CEM but not on the myeloid cell lines KG1 and K562. Finally, the presence of a chlorine atom in the alkyl-chloride derivatives **12o** and **12p** seemed to further improve the potency of these 1,2-FNQTs. Compound **12p** performed comparably to doxorubicin and even better than cisplatin, which are classical agents used in anticancer therapy.

Although all compounds of this series were cytotoxic to myeloid cell lines, the potency in myeloid cells was lower than in lymphoid cells and the compounds with stronger cytotoxicity were different for KG1 and K562. This is evidence for the higher resistance of AML to drugs in comparison with ALL [37,38] as well as the heterogeneity of myeloid leukemias [1,39].

1,2,3-1*H*-triazol has recently been identified as a general scaffold for generating glycosidase inhibitors because it was postulated to mimic the partial positive charge of the anomeric carbon of the reaction catalyzed by glycosidases [40–42] Glycosidases are involved in a variety of metabolic disorders and diseases such as diabetes, viral or bacterial infections, and cancer. Thus, the inhibition of these enzymes has many potential clinical applications [43–48].

It has been realized that the glycans expressed by cancer cells are either displayed at different levels or with different structures than those expressed by normal cells. Glycans regulate tumor proliferation, differentiation, invasion, metastasis, immune surveillance and angiogenesis. Altered glycosylation results in altered expression of cell surface oligosaccharides, protein folding, or stabilization of tertiary structures, resulting in defective recognition and elimination of glycoproteins by cell quality control mechanisms [49,50]. Hence, the incorporation of the 1,2,3-1*H*-triazol nucleus into the 1,2-FNQTs has improved the anticancer properties of such molecules. The anticancer effects may be a result of the observed glycosidase inhibition associated with the triazol scaffold.

2.4. Cytotoxic activity in normal peripheral blood mononuclear cells

To find compounds that presented potent cytotoxicity to leukemia cells and low toxicity to normal cells, we screened all compounds for cytotoxic activity in normal PBMCs from human donors at concentrations 10× higher than the respective IC_{50} found in leukemia cells. Such high concentrations were chosen to allow for rapid identification of compounds showing any potential cytotoxicity against normal cells. The majority of the compounds showed high toxicity (>80%) in this screening (data not shown) except for **12a**, **12b**, **12k** and **12o** (Fig. 5).

At 10 μM, a concentration that would kill nearly all leukemia cells (according to their IC_{50} values in Table 2), compounds **12a**, **12b**, **12k** and **12o** showed only a partial disruption of human donors' PBMC viability. Compound **12b** presented the lowest toxicity, reducing cell viability by only 30% on average (Fig. 5). The addition of a phenyl group to the triazol ring in **12b** led to a good compromise between cytotoxic potential and specificity.

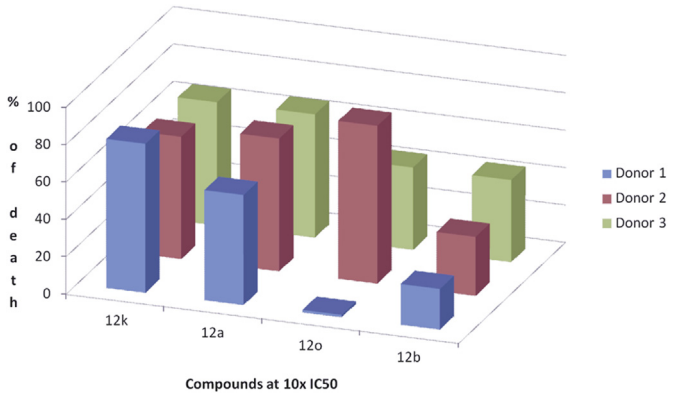

Fig. 5. Toxicity in normal PBMCs from three donors. Over 48 h, 5×10^4 PBMCs of donors were treated with compounds at doses 10× the IC_{50} determined in leukemia cell lines. Cytotoxicity was measured by AlamarBlue method.

Beta-lapachone, a natural 1,2-furanonaphthoquinone related to the parental compound of the series studied in this work, presented a similar level of toxicity with normal hematopoietic cells (IC_{50} = 14–16 μM, calculated from unstimulated PBMCs from 8 normal donors) [51]. Nor-beta-lapachone itself seems to be slightly less toxic considering its weak cytotoxicity against human lymphocytes (IC_{50} > 22 μM) and rodent V79 fibroblasts (IC_{50} = 13 μM) [27].

2.5. Predicted toxicity and other drug relevant properties

To anticipate any toxicity risks and evaluate the drug-like characteristics of the synthesized compounds, we computed a set of drug relevant properties from their 2D chemical structures (Table 3). The calculated properties indicated that most 1,2,3-triazole derivatives of nor-β-lapachone present a better toxicological profile than both their parent compound and the classical cytotoxic anticancer agent doxorubicin. To predict intestinal

Table 3
Predicted drug-relevant properties of the 1,2-furanonaphthoquinones tethered to 1,2,3-1*H*-triazoles.

Compounds	cLog*P*	Solubility [LogS(mol/L)]	TPSA (Å^2)	nON	nOH/NH	N violations[a]
Nor-b-Lapachone	2.36	−3.06	43.4	3	0	0
Doxorubicin	0.42	−4.66	206.1	12	7	3
10a	2.51	−3.39	94.3	7	1	0
10b	2.76	−3.39	74.1	6	0	0
12a	3.26	−3.89	74.1	6	0	0
12b	2.97	−3.88	74.1	6	0	0
12c	2.86	−3.9	83.3	7	0	0
12d	4.58	−5.38	74.1	6	0	1
12e	2.47	−2.90	74.1	6	0	0
12f	2.93	−3.17	74.1	6	0	0
12g	3.40	−3.44	74.1	6	0	0
12h	3.86	−3.71	74.1	6	0	0
12i	0.71	−2.01	94.3	7	1	0
12j	1.36	−2.49	94.3	7	1	0
12k	1.83	−2.76	94.3	7	1	0
12l	2.63	−3.19	94.3	7	1	0
12m	1.20	−2.42	100.4	8	0	0
12n	2.02	−3.04	92.6	8	0	0
12o	1.90	−3.24	74.1	6	0	0
12p	2.65	−3.30	74.1	6	0	0

[a] Number of violations to the Lipinski's "rule of five": log*P* ≤ 5, molecular weight ≤500, number of hydrogen bond acceptors ≤10, and number of hydrogen bond donors ≤5.

absorption, we estimated the molecular polar surface areas (PSA) of the triazol compounds from the calculated TPSA. PSA has been extensively used in medicinal chemistry for modeling absorption phenomena and to optimize a drug's ability to permeate cells. The PSA of a molecule is defined as the surface sum over all polar atoms, which primarily consist of oxygen and nitrogen as well as their attached hydrogens. The PSA of the triazol compounds suggested a better intestinal absorption (PSA < 140 $Å^2$) than doxorubicin (PSA = 206.1 $Å^2$). On the other hand, most triazol derivatives differ from nor-β-lapachone (PSA = 43.4 $Å^2$) in that they are unlikely to cross the blood–brain barrier (PSA > 60 $Å^2$). Molecules with a polar surface area greater than 140 $Å^2$ tend to be poor at permeating cell membranes, while a PSA of less than 60 $Å^2$ is usually needed for molecules to penetrate the blood–brain barrier and thus act on the brain and other central nervous system tissues [52]. Thus, the calculated PSA values for these hybrid nor-β-lapachone-triazol derivatives indicate a possible better oral bioavailability with a smaller chance of CNS toxicity.

Doxorubicin hydrochloride (Dox.HCl) is approved to be used alone or with other drugs to treat both ALL and AML (U.S. National Cancer Institute). However, Dox.HCl shows very low oral bioavailability (~5%) mainly due to its limited intestinal absorption [53] but also to other contributing factors that include substrate specificity to the P-glycoprotein (P-gp) efflux pump, acid catalyzed hydrolysis in the stomach, and susceptibility to cytochrome P450 (CYP450), resulting in high first-pass metabolism [54]. Therefore, only the injectable form of Dox.HCl is used in the clinic under the trade names Adriamycin® and Rubex® (Dox.HCl in solution form). Formulations designed to improve doxorubicin clinical efficacy exist, such as non-PEGylated (Myocet®) and PEGlyated liposomal formulations (Doxil®, Caelyx®, and LipoDox®), but their safety is still hampered by the well-known doxorubicin induced cardiotoxicity [55]. The latter is a result of a complex interplay of different mechanisms, whereas interference with iron metabolism and oxidative stress induced by doxorubicin-generated ROS are considered the primary mechanisms [56].

Computational prediction of the drug-relevant properties for nor-β-lapachone and its 1,2,3-1*H*-triazol hybrid derivatives indicated that many of the problems associated with doxorubicin may be absent or weaker in these compounds. For instance, admetSAR server results indicated that none of the most promising compounds revealed in this work (e.g., **12a**, **12b**, **12i**, **12k**, **12o** and **12p**) had been predicted with high probabilities to be substrates of P-gp or potent inhibitors of the Human Ether-a-go-go-Related Gene (hERG) (data not shown). P-gp is implicated in diminished intestinal absorption and drug-induced resistance in many cancers [57], while hERG is a potassium channel with critical importance to ventricular repolarization whose inhibition has been use as a major parameter for preclinical assessment of drug-induced ventricular arrhythmia [58].

3. Conclusion

In the present work, we synthesized a series of eighteen new 1,2-furanonaphthoquinones tethered to 1,2,3-1*H*-triazoles and investigated their antileukemic activity. The improved cytotoxic potential when compared with the parent nor-β-lapachone indicates that the attachment of a 1,2,3-1*H*-triazol to a variety of C-4 substituents mostly had a positive effect on the anticancer activity of the newly synthesized compounds.

Compound **12b** has great potential for further development as an anti-leukemia drug not only because of its potent and selective cytotoxicity (normal x cancer cells) but also because of its selectivity against leukemia lymphoid cell lines (approximately 7–19 times more effective than in leukemia myeloid cells). Additionally, compound **12p** is also promising due to its high cytotoxic activity against some leukemia cells (IC_{50} ranging from 0.48 to 1.38 μM) and its lower toxicity against normal hematopoietic cells (estimated IC_{50} > 10 μM). Compounds such as these could be the key to developing more effective therapies against leukemia with fewer side effects, especially for cases of resistance or relapse that prevent the improvement of survival rates in lymphoid leukemia.

4. Experimental section

4.1. Chemistry

Reagents were purchased from Sigma Aldrich Brazil LTDA and were used without further purification. Column chromatography was performed with silica gel 60 (Merck 70–230 mesh). Analytical thin-layer chromatography was performed with silica gel plates (Merck, TLC silica gel 60 F254) and the plots were visualized using UV light or aqueous solutions of ammonium sulfate. Yields refer to chromatographically and spectroscopically homogeneous materials. Melting points were obtained on a Fischer-Johns apparatus and were uncorrected. Infrared spectra were measured using KBr pellets on a Perkin–Elmer model 1420 FT-IR Spectrophotometer calibrated relative to the 1601.8 cm^{-1} absorbance of polystyrene. NMR spectra were recorded on a Varian Unity Plus VXR (500 MHz) instrument in DMSO-d_6 and $CDCl_3$ solutions. The chemical shift data were reported in units of δ (ppm) downfield from tetramethylsilane or the solvent, which were used as an internal standard. Coupling constants (J) are reported in Hertz and refer to apparent peak multiplicities. The high resolution mass spectra (electrospray ionization) were obtained using a QTOF Micro (Waters, Manchester, UK) mass spectrometer (HRESIMS).

4.1.1. General procedure for preparation of ***10a,b***, ***11*** and ***12a–p***

The general protocol for the synthesis of 2,2-dimethyl-3-(4-(alkyl or aryl)-1*H*-1,2,3-triazol-1-yl)-2,3-dihydronaphtho[1,2-*b*]furan-4,5-dione has been reported elsewhere [36]. Briefly, nor-β-lapachol (**7**) was reacted with excess of bromine in chloroform, followed by nucleophilic substitution with sodium azide in dichloromethane to yield **11** (3-azido-2,2-dimethyl-2,3-dihydronaphtho[1,2-b]furan-4,5-dione). This key intermediate was employed in Huisgen [59] 1,3-dipolar cyclization with an appropriate terminal alkyne catalyzed by copper (I) ion, also known as a click reaction [60], to obtain the 2,2-dimethyl-3-(4-(alkyl or aryl)-1*H*-1,2,3-triazol-1-yl)-2,3-dihydronaphtho[1,2-*b*]furan-4,5-dione **10a**,**b** and **12a–p** [61–63].

*4.1.1.1. 3-(4-(1-Hydroxycyclohexyl)-1H-1,2,3-triazol-1-yl)-2,2-dimethyl-2,3-dihydronaphtho[1,2-b]furan-4,5-dione (**10a**).* Compound **10a** was obtained in 58% yield as yellow solid; m.p. 100–101 °C. IR (KBr, cm^{-1}): ν 1651, 1590, 1574, 1494, 1410, 1257, 1222, 1160, 1084, 1051; ^{1}H NMR (DMSO-d_6, 500 MHz): δ 1.12 (3H, s), 1.40–1.36 (2H, m), 1.48–1.45 (2H, m), 1.78–1.57 (4H, m), 1.80 (3H, s), 2.03–1.95 (2H, m), 6.10 (1H, s), 7.88 (1H, d, J = 7.8 Hz), 7.97–7.90 (2H, m), 8.18 (1H, d, J = 6.9 Hz), 8.24 (1H, s); ^{13}C NMR (DMSO-d_6, 125 MHz): 20.3, 21.5, 25.0, 26.7, 37.6, 65.7, 67.6, 95.1, 111.0, 121.1, 124.7, 126.5, 128.4, 131.6, 132.7, 134.3, 155.1, 169.4, 174.3, 179.6.

*4.1.1.2. 3-(4-(Cyclohex-1-en-1-yl)-1H-1,2,3-triazol-1-yl)-2,2-dimethyl-2,3-dihydronaphtho[1,2-b]furan-4,5-dione (**10b**).* Compound **10b** was obtained in 48% yield as yellow solid; m.p. 187–188 °C. IR (KBr, cm^{-1}): ν 1650, 1612, 1567, 1410, 1216; ^{1}H NMR ($CDCl_3$, 500 MHz): δ 1.20 (3H, s), 1.61–1.66 (2H, m), 1.70–1.74 (2H, m), 1.74 (3H, s), 2.15–2.19 (2H, m), 2.31–2.33 (2H, m), 5.94 (1H, s), 6.50–6.52 (1H, m), 7.31 (1H, s), 7.72 (1H, dt, J = 1.5, 7.3 Hz), 7.75 (1H, dt, J = 1.5, 7.8 Hz), 7.80 (1H, dd, J = 1.0, 7.3 Hz), 8.18 (1H, dd, J = 1.5, 7.3 Hz); ^{13}C NMR

($CDCl_3$, 125 MHz): 21.0, 22.0, 22.2, 25.1, 26.1, 27.5, 66.5, 95.9, 111.2, 117.6, 125.3, 125.4, 126.7, 126.8, 129.7, 131.3, 133.1, 134.7, 149.1, 170.9, 174.4, 179.9; HRESIMS *m/z* 376.1658 $[M+H]^{+\bullet}$ (Calcd. for $C_{22}H_{22}N_3O_3^+$: 376.1656).

*4.1.1.3. 3-(4-Cyclohexyl-1H-1,2,3-triazol-1-yl)-2,2-dimethyl-2,3-dihydronaphtho[1,2-b]furan-4,5-dione (**12a**).* Compound **12a** was obtained in 52% yield as orange solid; m.p. 92–93 °C. IR (KBr, cm^{-1}): ν 3129, 2925, 1654, 1493, 1451, 1221; ^1H NMR ($CDCl_3$, 500 MHz): δ 1.09 (3H, s), 1.12–1.34 (6H, m), 1.57–1.70 (2H, m), 1.67 (3H, s), 1.92–1.94 (2H, m), 2.64–2.70 (1H, m), 5.86 (1H, s), 7.10 (1H, s), 7.65 (1H, dt, J = 1.5, 7.3 Hz), 7.69 (1H, dt, J = 1.5, 7.3 Hz), 7.73 (1H, dd, J = 1.5, 7.3 Hz), 8.12 (1H, dd, J = 1.5, 7.3 Hz); ^{13}C NMR ($CDCl_3$, 125 MHz): 20.8, 25.8, 25.9, 27.5, 29.5, 32.7, 32.8, 35.1, 66.7, 96.0, 111.3, 118.6, 125.4, 126.6, 129.8, 131.3, 133.1, 134.7, 153.4, 170.9, 174.4, 180.0; HRESIMS *m/z* 378.1809 $[M+H]^{+\bullet}$ (Calcd. for $C_{22}H_{24}N_3O_3^+$: 378.1812).

*4.1.1.4. 2,2-Dimethyl-3-(4-phenyl-1H-1,2,3-triazol-1-yl)-2,3-dihydronaphtho[1,2-b]furan-4,5-dione (**12b**).* Compound **12b** was obtained in 92% yield as yellow solid. m.p. 178–179 °C. IR (KBr, cm^{-1}): ν 3414, 2362, 2342, 1655, 1618, 1588, 1572, 1409, 1222, 768; ^1H NMR ($CDCl_3$, 500 MHz): δ 1.25 (3H, s), 1.78 (3H, s), 6.02 (1H, s), 7.30 (1H, s), 7.38 (2H, t, J = 7.3 Hz), 7.71–7.74 (2H, m), 7.75–7.79 (1H, m), 7.75–7.79 (1H, m), 7.75–7.79 (1H, m), 7.82 (1H, d, J = 7.3 Hz), 8.20 (1H, d, J = 7.3 Hz); ^{13}C NMR ($CDCl_3$, 125 MHz): 21.0, 27.6, 66.8, 95.9, 111.1, 118.8, 125.6, 126.5, 128.1, 128.6, 129.9, 130.0, 131.4, 125.5, 133.3, 134.8, 147.5, 171.1, 174.4, 179.9; HRESIMS *m/z* 372.1359 $[M+H]^{+\bullet}$ (Calcd. for $C_{22}H_{18}N_3O_3^+$: 372.1343).

*4.1.1.5. 3-(4-(4-Methoxyphenyl)-1H-1,2,3-triazol-1-yl)-2,2-dimethyl-2,3-dihydronaphtho[1,2-b]furan-4,5-dione (**12c**).* Compound **12c** was obtained in 56% yield as yellow solid; m.p. 128–129 °C. IR (KBr, cm^{-1}): ν 1657, 1618, 1572, 1497, 1411, 1252, 1225, 1178, 1085, 1030; ^1H NMR ($CDCl_3$, 500 MHz): δ 1.24 (3H, s), 1.77 (3H, s), 3.81 (3H, s), 6.00 (1H, s), 6.90 (2H, d, J = 8.8 Hz), 7.62 (1H, s), 7.70 (2H, d, J = 8.8 Hz), 7.71–7.74 (1H, m), 7.76 (1H, dt, J = 1.5, 7.8 Hz), 7.82 (1H, dd, J = 1.5, 7.8 Hz), 8.19 (1H, dd, J = 1.5, 7.8 Hz); ^{13}C NMR ($CDCl_3$, 125 MHz): 21.0, 27.5, 55.1, 66.7, 95.9, 111.2, 114.0, 118.2, 122.8, 125.4, 126.5, 126.9, 129.7, 131.3, 133.2, 134.7, 147.3, 159.5, 171.1, 174.4, 180.0; HRESIMS *m/z* 402.1452 $[M+H]^{+\bullet}$ (Calcd. for $C_{23}H_{20}N_3O_4^+$: 402.1448).

*4.1.1.6. 2,2-Dimethyl-3-(4-(4-pentylphenyl)-1H-1,2,3-triazol-1-yl)-2,3-dihydronaphtho[1,2-b]furan-4,5-dione (**12d**).* Compound **12d** was obtained in 65% yield as yellow solid; m.p. 161–162 °C. IR (KBr, cm^{-1}): ν 2929, 1656, 1616, 1571, 1588, 1414, 1222, 777; ^1H NMR ($CDCl_3$, 500 MHz): δ 0.87 (3H, t, J = 6.8 Hz), 1.24 (3H, s), 1.28–1.36 (4H, m), 1.57–163 (2H, m), 1.77 (3H, s), 2.59 (2H, t, J = 7.34 Hz), 6.01 (1H, s), 7.19 (2H, d, J = 7.8 Hz), 7.69–7.74 (2H, m), 7.69–7.74 (1H, m), 7.69–7.74 (1H, m), 7.76 (1H, dt, J = 1.0, 7.3 Hz), 7.82 (1H, dd, J = 1.0, 7.3 Hz), 8.19 (1H, dd, J = 1.5, 7.8 Hz); ^{13}C NMR ($CDCl_3$, 125 MHz): 14.0, 21.2, 22.5, 27.7, 31.0, 31.4, 35.7, 66.9, 96.0, 111.3, 118.8, 125.6, 125.7, 126.7, 127.6, 128.8, 129.9, 131.5, 133.3, 134.8, 143.2, 147.7, 171.2, 174.6, 180.1; HRESIMS *m/z* 442.2128 $[M+H]^{+\bullet}$ (Calcd. for $C_{27}H_{28}N_3O_3^+$: 442.2125).

*4.1.1.7. 2,2-Dimethyl-3-(4-propyl-1H-1,2,3-triazol-1-yl)-2,3-dihydronaphtho[1,2-b]furan-4,5-dione (**12e**).* Compound **12e** was obtained in 80% yield as yellow solid. m.p. 219–220 °C. IR (KBr, cm^{-1}): ν 3412, 3123, 1651, 1611, 1586, 1567, 1411, 1219, 779; ^1H NMR ($CDCl_3$, 500 MHz): δ 0.85 (3H, t, J = 7.3 Hz), 1.11 (3H, s), 1.58 (2H, q, J = 7.3 Hz), 1.67 (3H, s), 2.58 (2H, td, J = 1.9, 7.3 Hz), 5.86 (1H, s), 7.15 (1H, s), 7.63–7.74 (1H, m), 7.63–7.74 (1H, m), 7.63–7.74 (1H, m), 8.11 (1H, dd, J = 1.5, 7.3 Hz); ^{13}C NMR ($CDCl_3$, 125 MHz): 13.6, 20.9, 22.5, 27.5, 27.6, 66.6, 96.0, 111.4, 120.3, 126.7, 129.8, 131.4, 125.5, 133.3, 134.9, 148.1, 171.1, 174.6, 180.1; HRESIMS *m/z* 338.1502 $[M+H]^{+\bullet}$ (Calcd. for $C_{19}H_{20}N_3O_3^+$: 338.1499).

*4.1.1.8. 3-(4-Butyl-1H-1,2,3-triazol-1-yl)-2,2-dimethyl-2,3-dihydronaphtho[1,2-b]furan-4,5-dione (**12f**).* Compound **12f** was obtained in 90% yield as yellow solid; m.p. 219–220 °C. IR (KBr, cm^{-1}): ν 3.128, 3.077, 2.957, 2.930, 2.850, 1.657, 1.621, 1.589, 1.572, 1.408, 1.221, 776; ^1H NMR (DMSO-d_6, 500 MHz): δ 0.86 (3H, t, J = 7.2 Hz), 1.01 (3H, s), 1.29 (2H, dt, J = 7.2, 14.9 Hz), 1.58–1.52 (2H, m), 1.68 (3H, m), 1.68 (3H, s), 2.59 (2H, dt, 2.2, 7.7 Hz), 5,96 (1H, s), 7,88–7,75 (3H, m), 8.05 (1H, s), 8.07 (1H, s); ^{13}C NMR (DMSO, 125 MHz): 13.5, 21.5, 21.8, 22.4, 23.6, 30.8, 92.8, 110.8, 118.5, 124.8, 126.0, 128.9, 132.5, 134.7, 135.2, 172.5, 178.9, 185.6, 197.2; HRESIMS *m/z* 352.1651 $[M+H]^{+\bullet}$ (Calcd. for $C_{20}H_{21}N_3O_3^+$: 351.1583).

*4.1.1.9. 2,2-Dimethyl-3-(4-pentyl-1H-1,2,3-triazol-1-yl)-2,3-dihydronaphtho[1,2-b]furan-4,5-dione (**12g**).* Compound **12g** was obtained in 70% yield as yellow solid; m.p. 65–66 °C. IR (KBr, cm^{-1}): ν 3.128, 3.079, 2.955, 2.930, 2.859, 1.657, 1.621, 1589, 1.572, 1.409, 1.222, 776; ^1H NMR (DMSO-d_6, 500 MHz): δ 0.83 (3H, t, 7.0 Hz), 1.30–1.23 (4H, m), 1.61–1.53 (2H, m), 2.60–2.55 (2H, m), 3.31 (6H, s), 5.97 (1H, s), 7.77–7.74 (1H, m), 7.81–7.82 (1H, m), 7.87–7.82 (1H, m), 8.05 (1H, dd, 7.3 and 1.5 Hz); 8.06 (1H, s); ^{13}C NMR (DMSO, 125 MHz): 13.7, 21.7, 22.0, 22.4, 28.3, 30.6, 92.8, 124.8, 128.9, 132.5, 134.7, 135.2, 172,5, 185.6, 197.2; HRESIMS *m/z* 366.1813 $[M+H]^{+\bullet}$ (Calcd. for $C_{21}H_{23}N_3O_4^+$: 365.4256).

*4.1.1.10. 3-(4-Hexyl-1H-1,2,3-triazol-1-yl)-2,2-dimethyl-2,3-dihydronaphtho[1,2-b]furan-4,5-dione (**12h**).* Compound **12h** was obtained in 88% yield as yellow solid; m.p. 178–179 °C. IR (KBr, cm^{-1}): ν 2927, 1654, 1620, 1588, 1568, 1409, 1218, 1112; ^1H NMR ($CDCl_3$, 500 MHz): δ 0.85 (3H, t, J = 7.2 Hz), 1.17 (3H, s), 1.23–1.32 (2H, m), 1.23–1.32 (2H, m), 1.23–1.32 (2H, m), 1.62 (2H, t, J = 7.2 Hz), 1.74 (3H, s), 2.66 (2H, t, J = 7.2 Hz), 5.93 (1H, s), 7.21 (1H, s), 7.69–7.80 (1H, m), 7.69–7.80 (1H, m), 7.69–7.80 (1H, m), 8.18 (1H, d, J = 7.7 Hz); ^{13}C NMR ($CDCl_3$, 125 MHz): 13.8, 20.8, 22.3, 25.4, 27.5, 28.6, 29.1, 31.3, 66.4, 95.9, 111.2, 120.0, 126.6, 129.7, 131.3, 125.4, 133.1, 134.7, 148.2, 170.9, 174.4, 179.9; HRESIMS *m/z* 380.1973 $[M+H]^{+\bullet}$ (Calcd. for $C_{22}H_{26}N_3O_3^+$: 380.1969).

*4.1.1.11. 3-(4-(Hydroxymethyl)-1H-1,2,3-triazol-1-yl)-2,2-dimethyl-2,3-dihydronaphtho[1,2-b]furan-4,5-dione (**12i**).* Compound **12i** was obtained in 88% yield as yellow solid; m.p. 212–213 °C. IR (KBr, cm^{-1}): ν 3626, 1652, 1614, 1584, 1567, 1416, 1218, 795; ^1H NMR ($CDCl_3$, 500 MHz): δ 1.21 (3H, s), 1.76 (3H, s), 4.77 (2H, s), 5.97 (1H, s), 7.50 (1H, s), 7.73–7.81 (1H, m), 7.73–7.81 (1H, m), 7.73–7.81 (1H, m), 8.10 (1H, d, J = 7.3 Hz); ^{13}C NMR ($CDCl_3$, 125 MHz): 22.5, 27.0, 55.1, 66.0, 95.2, 111.3, 122.9, 126.6, 128.7, 131.9, 124.9, 132.9, 134.6, 148.0, 169.7, 174.6, 179.8; HRESIMS *m/z* 326.1136 $[M+H]^{+\bullet}$ (Calcd. for $C_{17}H_{16}N_3O_4^+$: 326.1135).

*4.1.1.12. 3-(4-(2-Hydroxypropan-2-yl)-1H-1,2,3-triazol-1-yl)-2,2-dimethyl-2,3-dihydronaphtho[1,2-b]furan-4,5-dione (**12j**).* Compound **12j** was obtained in 83% yield as yellow solid; m.p. 220–221 °C. IR (KBr, cm^{-1}): ν 3422, 2981, 2968, 2925, 1657, 1615, 1588, 1570, 1412, 1224, 780; ^1H NMR ($CDCl_3$, 500 MHz): δ 1.17 (3H, s), 1.60 (6H, s), 1.75 (3H, s), 5.95 (1H, s), 7.38 (1H, s), 7.70–7.80 (1H, m), 7.70–7.80 (1H, m), 7.70–7.80 (1H, m), 8.17 (1H, d, J = 7.9 Hz); ^{13}C NMR ($CDCl_3$, 125 MHz): 21.5, 27.7, 30.5, 30.6, 66.8, 68.8, 96.2, 111.4, 118.7, 126.7, 130.6, 131.5, 125.6, 133.4, 134.9, 155.7, 171.3, 174.6, 180.1; HRESIMS *m/z* 354.1447 $[M+H]^{+\bullet}$ (Calcd. for $C_{19}H_{20}N_3O_4^+$: 354.1448).

*4.1.1.13. 3-(4-(2-Hydroxybutan-2-yl)-1H-1,2,3-triazol-1-yl)-2,2-dimethyl-2,3-dihydronaphtho[1,2-b]furan-4,5-dione (**12k**).*

Compound **12k** was obtained in 90% yield as yellow solid; m.p. 193–195 °C. IR (KBr, cm^{-1}): ν 3416, 2970, 1656, 1615, 1570, 1570, 1411, 1223, 778; ^{1}H NMR ($CDCl_3$, 500 MHz): δ 0.80 (3H, dd, J = 5.4, 7.9 Hz), 1.17 (3H, s), 1.54 (3H, d, J = 5.4 Hz), 1.75 (3H, s), 1.80–1.92 (2H, m), 5.95 (1H, d, J = 11.5 Hz), 7.37 (1H, d, J = 3.0 Hz), 7.70–7.81 (1H, m), 7.70–7.81 (1H, m), 7.70–7.81 (1H, m), 8.17 (1H, d, J = 7.3 Hz); ^{13}C NMR ($CDCl_3$, 125 MHz): 8.1, 20.9, 22.9, 27.5, 35.7, 66.6, 71.3, 96.0, 111.2, 119.5, 126.5, 129.8, 131.4, 125.5, 133.2, 134.7, 154.3, 171.1, 174.4, 180.0; HRESIMS m/z 368.1608 $[M+H]^{+\bullet}$ (Calcd. for $C_{20}H_{22}N_3O_4^+$: 368.1605).

*4.1.1.14. 3-(4-(2-Hydroxy-4-methylpentan-2-yl)-1H-1,2,3-triazol-1-yl)-2,2-dimethyl-2,3-dihydronaphtho[1,2-b]furan-4,5-dione (**12l**).* Compound **12l** was obtained in 77% yield as yellow solid; m.p. 163–164 °C. IR (KBr, cm^{-1}): ν 3128, 3077, 2957, 2930, 2850, 1657, 1621, 1589, 1572, 1408, 1221, 776; ^{1}H NMR (DMSO, 500 MHz): δ 0.70 (3H, dd, J = 2.9, 6.4 Hz), 0.78 (3H, dd, J = 2.9, 6.4 Hz), 1.02 (3H, s), 1.43 (3H, d, J = 5.3 Hz), 1.54–1.67 (3H, m), 1.69 (3H, d, J = 5.3 Hz), 6.00 (1H, d, J = 6.4 Hz), 7.75–7.85 (3H, m), 8.04 (1H, s), 8.06 (1H, s); ^{13}C NMR (DMSO-d_6, 125 MHz): 20.4, 20.5, 23.6, 23.6, 24.0, 24.1, 24.2, 24.3, 26.8, 26.9, 29.4, 29.5, 51.3, 51.4, 65.8, 65.9, 69.7, 69.9, 95.0, 95.1, 111.0, 111.3, 121.2, 121.3, 124.7, 124.8, 126.5, 126.6, 128.4, 128.5, 131.7, 131.8, 132.7, 132.8, 134.4, 134.5, 155.0, 155.1, 169.4, 169.5, 174.4, 174.5, 179.6, 179.7; HRESIMS m/z 396.1923 $[M+H]^{+\bullet}$ (Calcd. for $C_{19}H_{20}N_3O_4^+$: 395.1845).

*4.1.1.15. (1-(2,2-Dimethyl-4,5-dioxo-2,3,4,5-tetrahydronaphtho[1,2-b]furan-3-yl)-1H-1,2,3-triazol-4-yl)methyl acetate (**12m**).* Compound **12m** was obtained in 75% yield as yellow solid; m.p. 183–185 °C. IR (KBr, cm^{-1}): ν 3147, 1747, 1623, 1561, 1554, 1405, 1240, 1221, 1035, 782; ^{1}H NMR ($CDCl_3$, 500 MHz): δ 1.17 (3H, s), 1.75 (3H, s), 2.04 (3H, s), 5.16 (2H, s), 5.96 (1H, s), 7.55 (1H, s), 7.70–7.80 (1H, m), 7.70–7.80 (1H, m), 7.70–7.80 (1H, m), 8.18 (1H, dd, J = 1.5, 7.3 Hz); ^{13}C NMR ($CDCl_3$, 125 MHz): 20.6, 21.0, 27.5, 57.3, 66.7, 95.7, 110.9, 123.2, 126.4, 129.7, 131.3, 125.4, 133.2, 134.7, 142.5, 170.7, 171.2, 174.3, 179.8; HRESIMS m/z 368.1245 $[M+H]^{+\bullet}$ (Calcd. for $C_{19}H_{18}N_3O_5^+$: 368.1241).

*4.1.1.16. 2,2-Dimethyl-3-(4-(((tetrahydro-2H-pyran-2-yl)oxy)methyl)-1H-1,2,3-triazol-1-yl)-2,3-dihydronaphtho[1,2-b]furan-4,5-dione (**12n**).* Compound **12n** was obtained in 98% yield as yellow solid; m.p. 139–140 °C. IR (KBr, cm^{-1}): ν 2943, 1664, 1625, 1589, 1573, 1410, 1221, 1118, 1028, 779; ^{1}H NMR ($CDCl_3$, 500 MHz): δ 1.13 (3H, s), 1.42–1.65 (6H, m), 1.69 (3H, s), 3.41–3.46 (1H, m), 3.75–3.80 (1H, m), 4.55–4.79 (3H, m), 5.81 (1H, s), 5.89 (1H, s), 5.90 (1H, s), 7.41 (1H, s), 7.42 (1H, s), 7.69 (3H, m), 8.11 (1H, dt, J = 1.5, 7.3 Hz), 8.12 (1H, dt, J = 1.5, 7.3 Hz); ^{13}C NMR ($CDCl_3$, 125 MHz): 19.2, 19.3, 23.0, 24.8, 25.3, 27.7, 30.3, 30.4, 60.5, 60.6, 62.3, 62.4, 66.7, 66.8, 95.9, 96.0, 111.2, 111.3, 125.5, 126.6, 129.9, 130.3, 131.5, 133.3, 134.8, 135.1, 171.2, 171.3, 174.5, 174.6, 180.0; HRESIMS m/z 410.1706 $[M+H]^{+\bullet}$ (Calcd. for $C_{22}H_{22}N_3O_5^+$: 410.1710).

*4.1.1.17. 3-(4-(Chloromethyl)-1H-1,2,3-triazol-1-yl)-2,2-dimethyl-2,3-dihydronaphtho[1,2-b]furan-4,5-dione (**12o**).* Compound **12o** was obtained in 79% yield as yellow solid; m.p. 212–213 °C. IR (KBr, cm^{-1}): ν 1655, 1614, 1586, 1568, 1412, 1218; ^{1}H NMR ($CDCl_3$, 500 MHz): δ 1.14 (3H, s), 1.70 (3H, s), 4.60 (2H, m), 5.91 (1H, s), 7.49 (1H, d, J = 4.4 Hz), 7.66–7.75 (1H, m), 7.66–7.75 (1H, m), 7.66–7.75 (1H, m), 8.12 (1H, dd, J = 0.9, 7.3 Hz); ^{13}C NMR ($CDCl_3$, 125 MHz): 21.0, 27.5, 35.8, 66.8, 95.8, 110.8, 122.3, 126.4, 129.8, 131.3, 125.5, 133.3, 134.7, 144.5, 171.2, 174.4, 179.9; HRESIMS m/z 344.0792 $[M+H]^{+\bullet}$ (Calcd. for $C_{17}H_{15}ClN_3O_3^+$: 344.0796).

*4.1.1.18. 3-(4-(3-Chloropropyl)-1H-1,2,3-triazol-1-yl)-2,2-dimethyl-2,3-dihydronaphtho[1,2-b]furan-4,5-dione (**12p**).* Compound **12p** was obtained in 86% yield as yellow solid; m.p. 63–64 °C. IR (KBr, cm^{-1}): ν 1643, 1570, 1492, 1408, 1219, 1173, 1083; ^{1}H NMR (DMSO-d_6, 500 MHz): δ 1.03 (3H, s), 1.69 (3H, s), 2.01–2.06 (2H, m), 2.74 (2H, t, J = 7.3 Hz), 3.63 (2H, dt, J = 2.4, 6.3 Hz), 5.98 (1H, s), 7.76–7.85 (3H, m), 8.06 (1H, d, J = 6.8 Hz), 8.10 (1H, s); ^{13}C NMR (DMSO-d_6, 125 MHz): 22.4, 22.8, 31.5, 44.5, 88.0, 92.7, 110.8, 121.8, 124.7, 126.0, 128.8, 129.8, 132.5, 134.6, 135.2, 172.5, 178.5, 185.5, 197.1; HRESIMS m/z 372.1097 $[M+H]^{+\bullet}$ (Calcd. for $C_{19}H_{18}ClN_3O_3^+$: 371.1037).

4.2. Biology

4.2.1. Leukemia cell lines

A panel of human leukemia cell lines that included myeloid (K562, KG1) and lymphoid cells (MOLT-4, CCRF-CEM) was used. Cell lines were obtained from ATCC (Philadelphia, PA, USA) and cultured in RPMI 1640 medium (Sigma–Aldrich®) supplemented with 10% inactivated fetal bovine serum (Sigma–Aldrich®) and 50 μg/ml gentamicin at 37 °C in a humidified incubator with 5% CO_2.

4.2.2. Normal peripheral blood mononuclear cells

Peripheral blood mononuclear cells (PBMCs) were isolated by density gradient centrifugation (Hystopaque; Sigma) from buffy coat preparations from healthy donors (C.E. Fiocruz protocol number 535/09). PBMCs were counted and seeded in 96-well plates with RPMI 1640 (Sigma–Aldrich®) supplemented with 10% inactivated fetal bovine serum.

The compounds were tested at a concentration 10× higher than their IC_{50} determined in leukemia cell lines.

4.2.3. Hemolysis assay

This assay was performed using fresh lamb blood from CECAL/Fiocruz (Breeding center of laboratory animals). Erythrocytes were collected by centrifugation at 1500 rpm for 15 min, washed three times with Phosphate buffered saline (PBS) with 10 mM of glucose at pH 7.4 and counted in a Countess®Automated Cell Counter (Life Technologies). Erythrocytes were seeded in 96-well plates at a concentration of 4×10^8/well in triplicate, and 10 μL of the compounds were added at a final concentration of 1000 μM in glucose-PBS (100 μL final volume). Ten microliters of PBS was used as a negative control (0% hemolysis) and 10 μL of Milli-Q H_2O was used as a positive control (100% hemolysis). The solutions were mixed and incubated in a shaker for 10 min at room temperature. After centrifugation at 13,000 rpm for 15 min, hemolysis was measured by reading the supernatant absorbance at 540 nm on a FlexStation 3 Benchtop Multi-Mode Microplate Reader (Molecular Devices, Sunnyvale, CA). All hemolysis data points were presented as the percentage of the complete hemolysis control obtained by osmotic shock with deionized water.

4.2.4. Cytotoxic activity

Leukemia cell lines and normal PBMCs were seeded in 96-well microculture plates and incubated for 48 h with the studied compounds before *in vitro* cytotoxicity was assessed using the AlamarBlue® kit (Life Technologies). This kit is based on the principle that only viable cells are able to reduce Resazurin, a blue reagent present in AlamarBlue®, to a pink colored and highly red fluorescent product, Resorufin, which can be spectrophotometrically quantitated using λ_{ex} = 560 nm and λ_{em} = 590 nm. For each cell or cell line used, an optimal time and number of cells were standardized for the incubation step with AlamarBlue® (Table 1). AlamarBlue® was added to cells at different times according to the optimal incubation times listed in Table 1 before the 48 h total incubation time was complete. Each of the 19 compounds was tested in triplicate wells at six or seven different concentrations varying from 0.01 μM to 200 μM (5 times lower than the highest

concentration tested in erythrocyte hemolysis). Control wells, which were used to determine 100% cell survival, contained only leukemic cells, culture medium and vehicle (up to 1% DMSO). The IC_{50} value, which is the drug concentration needed to kill 50% of the cells, was used as a measure of cytotoxicity. This was calculated using Sigmaplot 12.0 software (Systat Software Inc, Chicago, IL).

4.3. Computational prediction of toxicity and drug relevant properties

Calculations of cLogP and solubility were conducted using OSIRIS Property Explorer [64] web server at http://www.cheminformatics.ch/. Calculations of Topological Polar Surface Area (TPSA), number of hydrogen bond acceptor (nON) and donor (nNH/OH) atoms, and any violations to the Lipinski's "rule of five" ($\log P \leq 5$, molecular weight $\leq$500, number of hydrogen bond acceptors $\leq$10, and number of hydrogen bond donors $\leq$5 [65]; were performed using the MIPC server at http://www.molinspiration.com/cgi-bin/properties. Further predictions from the 2D chemical structure of ADMET (Absorption, Distribution and Metabolism) and toxic properties were performed within the admetSAR web server at http://www.admetexp.org [66].

Acknowledgments

Fellowships granted by CNPq, CAPES and FAPERJ are gratefully acknowledged. This work was partially supported by Capes grant number 058862/2010 and CNPq-FAPERJ-PRONEX grant number E-26/110.574/2010. We thank the Hemotherapy Service of the Hospital Clementino Fraga Filho (Federal University of Rio de Janeiro, Brazil) for providing buffy coats.

Appendix A. Supplementary data

Supplementary data related to this article can be found at http://dx.doi.org/10.1016/j.ejmech.2014.07.079.

References

[1] M. Greaves, Childhood leukaemia, Br. Med. J. 324 (2002) 283–287.
[2] D.G. Gilliland, Hematologic malignancies, Curr. Opin. Hematol. 8 (2001) 189–191.
[3] F. Schneider, S.K. Bohlander, S. Schneider, C. Papadaki, P. Kakadyia, A. Dufour, S. Vempati, M. Unterhalt, M. Feuring-Buske, C. Buske, J. Braess, H. Wandt, W. Hiddemann, K. Spiekermann, AML1-ETO meets JAK2: clinical evidence for the two hit model of leukemogenesis from a myeloproliferative syndrome progressing to acute myeloid leukemia, Leukemia 21 (2007) 2199–2201.
[4] C.H. Pui, W.E. Evans, Acute lymphoblastic leukemia, N. Engl. J. Med. 339 (1998) 605–615.
[5] A. Reiter, M. Schrappe, W.D. Ludwig, W. Hiddemann, S. Sauter, G. Henze, M. Zimmermann, F. Lampert, W. Havers, D. Niethammer, Chemotherapy in 998 unselected childhood ALL patients: results and conclusions of the multicenter trial ALL-BFM 86, Blood 84 (1994) 3122–3133.
[6] R.F. Stevens, I.M. Hann, K. Wheatley, R.G. Gray, Marked improvements in outcome with chemotherapy alone in paediatric acute myeloid leukemia: results of the United Kingdom Medical Research Council's 10th AML trial, Br. J. Haematol. 1010 (1998) 130–140.
[7] U. Creutzig, M. Zimmermann, J. Ritter, G. Henze, N. Graf, H. Löffler, G. Schellong, Definition of a standard risk group in children with AML, Br. J. Haematol. 104 (1999) 630–639.
[8] Y. Ravindranath, A.M. Yeager, M.N. Chang, C.P. Steuber, J. Krischer, J. Graham-Pole, A. Carroll, S. Inoue, B. Camitta, H.J. Weinstein, Autologous bone marrow transplantation versus intensive consolidation chemotherapy for acute myeloid leukemia in childhood. Pediatric Oncology Group, N. Engl. J. Med. 334 (1996) 1428–1434.
[9] R. Pieters, W.L. Carroll, Biology and treatment of acute lymphoblastic leucemia, Hematol. Oncol. Clin. N. Am. 24 (2010) 1–18.
[10] N. Howlader, M. Krapcho, J. Garshell, N. Neyman, S.F. Altekruse, C.L. Kosary, M. Yu, J. Ruhl, Z. Tatalovich, H. Cho, A. Mariotto, D.R. Lewis, H.S. Chen, E.J. Feuer, K.A. Cronin (Eds.), SEER Cancer Statistics Review, 1975–2010, National Cancer Institute. Bethesda, MD, http://seer.cancer.gov/csr/1975_2010/, based on November 2012 SEER data submission, posted to the SEER web site, April 2013.
[11] M. Rebucci, C. Michiels, Molecular aspects of cancer cell resistance to chemotherapy, Biochem. Pharmacol. 85 (2013) 1219–1226.
[12] J.J. Marin, O. Briz, M.J. Monte, A.G. Blazquez, R.I. Macias, Genetic variants in genes involved in mechanisms of chemoresistance to anticancer drugs, Curr. Cancer Drug Targets 12 (2012) 402–438.
[13] M. Gerlinger, A.J. Rowan, S. Horswell, J. Larkin, D. Endesfelder, E. Gronroos, P. Martinez, N. Matthews, A. Stewart, P. Tarpey, I. Varela, B. Phillimore, S. Begum, N.Q. McDonald, A. Butler, D. Jones, K. Raine, C. Latimer, C.R. Santos, M. Nohadani, A.C. Eklund, B. Spencer-Dene, G. Clark, L. Pickering, G. Stamp, M. Gore, Z. Szallasi, J. Downward, P.A. Futreal, C. Swanton, Intratumor heterogeneity and branched evolution revealed by multiregion sequencing, N. Engl. J. Med. 366 (2012) 883–892.
[14] P.R.R. Costa, Natural products as starting point for the discovery of new bioactive compounds: drug candidates with antiophidic, anticancer and antiparasitic properties, Rev. Virtual Quím. 1 (2009) 58–66.
[15] M.N. da Silva, V.F. Ferreira, M.C.B.V. de Souza, An overview of the chemistry and pharmacology of naphthoquinones with emphasis on b-lapachone and derivatives, Quim. Nova 26 (2003) 407–416.
[16] D.A. Boothman, D.K. Trask, A.B. Pardee, Inhibition of potentially lethal DNA damage repair in human tumor cells by beta-lapachone, an activator of topoisomerase I, Cancer Res. 49 (1989) 605–612.
[17] R.D. Anderson, N.A. Berger, International Commission for Protection against Environmental Mutagens and Carcinogens, Mutagenicity and carcinogenicity of topoisomerase-interactive agents, Mutat. Res. 309 (1994) 109–142.
[18] T.J. Monks, D.C. Jones, The metabolism and toxicity of quinones, quinonimines, quinone methides, and quinone-thioethers, Curr. Drug Metab. 3 (2002) 425–438.
[19] E.J. Park, K.S. Choi, T.K. Kwon, β-Lapachone-induced reactive oxygen species (ROS) generation mediates autophagic cell death in glioma U87 MG cells, Chem. Biol. Interact. 189 (2011) 37–44.
[20] Y.C. Lien, H.N. Kung, K.S. Lu, C.J. Jeng, Y.P. Chau, Involvement of endoplasmic reticulum stress and activation of MAP kinases in beta-lapachone-induced human prostate cancer cell apoptosis, Histol. Histopathol. 23 (2008) 1299–1308.
[21] E.A. Bey, M.S. Bentle, K.E. Reinicke, Y. Dong, C.R. Yang, L. Girard, J.D. Minna, W.G. Bornmann, J. Gao, D.A. Boothman, An NQO1- and PARP-1-mediated cell death pathway induced in non-small-cell lung cancer cells by beta-lapachone, Proc. Natl. Acad. Sci. U. S. A. 104 (2007) 11832–11837.
[22] S.B. Ferreira, D.T.G. Gonzaga, W.C. Santos, K.G.L. Araújo, V.F. Ferreira, Beta-lapachone: medicinal chemistry significance and structural modifications, Rev. Virtual Quím. 2 (2010) 140–160.
[23] J.R. Gómez Castellanos, J.M. Prieto, M. Heinrich, Red Lapacho (*Tabebuia impetiginosa*) – a global ethnopharmacological commodity? J. Ethnopharmacol. 121 (2009) 1–13.
[24] H. Hussain, K. Krohn, V.U. Ahmad, G.A. Miana, I.R. Greend, Lapachol: an overview, Ark. Part II (2007) 145–171.
[25] O.K. Eyong, P.S. Kumar, V. Kuete, G.N. Folefoc, E.A. Nkengfack, S. Baskaran, Semisynthesis and antitumoral activity of 2-acetylfuranonaphthoquinone and other naphthoquinone derivatives from lapachol, Bioorg. Med. Chem. Lett. 18 (2008) 5387–5390.
[26] S.C. Hooker, The constitution of lapachol and its derivatives. Part IV. 1 oxidation with potassium permanganate, J. Am. Chem. Soc. 58 (1936) 1168–1173.
[27] K.O. Eyong, M. Puppala, P.S. Kumar, M. Lamshöft, G.N. Folefoc, M. Spiteller, S. Baskaran, A mechanistic study on the Hooker oxidation: synthesis of novel indane carboxylic acid derivatives from lapachol, Org. Biomol. Chem. 11 (2013) 459–468.
[28] V.P. Glazunov, D.V. Berdyshev, A.Y. Yakubovskaya, N.D. Pokh, Chemistry of naphthazarin derivatives 13. Conformational analysis of 3-(alk-1-enyl)-2-hydroxy-1,4-naphthoquinones by quantum chemistry methods, Russ. Chem. Bull. Int. Ed. 55 (2006) 1729–1736.
[29] B.C. Cavalcanti, F.W.A. Barros, I.O. Cabral, J.R.O. Ferreira, H.I.F. Magalhães, H.V.N. Júnior, E.N. da Silva Júnior, F.C. de Abreu, C.O. Costa, M.O.F. Goulart, M.O. Moraes, C. Pessoa, Preclinical genotoxicology of nor-beta-lapachone in human cultured lymphocytes and Chinese Hamster lung fibroblasts, Chem. Res. Toxicol. 24 (2011) 1560–1574.
[30] E.N. da Silva Junior, C.F. de Deus, B.C. Cavalcanti, C. Pessoa, L.V. Costa-Lotufo, R.C. Montenegro, M.O. de Moraes, M.C.F.R. Pinto, C.A. de Simone, V.F. Ferreira, M.O.F. Goulart, C.K.Z. Andrade, A.V. Pinto, 3-Arylamino and 3-Alkoxy-nor-Beta-lapachone derivatives: synthesis and cytotoxicity against Cancer cell lines, J. Med. Chem. 53 (2010) 504–508.
[31] E.N. da Silva Júnior, M.C.B.V. de Souza, A.V. Pinto, M.C.F.R. Pinto, M.O.F. Goulart, F.W.A. Barros, C. Pessoa, L.V. Costa-Lotufo, R.C. Montenegro, M.O. de Moraes, V.F. Ferreira, Synthesis and potent antitumor activity of new arylamino derivatives of nor-beta-lapachone and nor-alfa-lapachone, Bioorg. Med. Chem. 15 (2007) 7035–7041.
[32] R. Inagaki, M. Ninomiya, K. Tanaka, K. Watanabe, M. Koketsu, Synthesis and cytotoxicity on human leukemia cells of furonaphthoquinones isolated from tabebuia plants, Chem. Pharm. Bull. 61 (2013) 670–673.
[33] S.G. Agalave, S.R. Maujan, V.S. Pore, Click chemistry: 1,2,3-triazoles as pharmacophores, Chem. Asian J. 6 (2011) 2696–2718.
[34] V.F. Ferreira, D.R. da Rocha, F.C. da Silva, P.G. Ferreira, N.A. Boechat, J.L. Magalhães, Novel 1H-1,2,3-, 2H-1,2,3-, 1H-1,2,4- and 4H-1,2,4-triazole derivatives: a patent review (2008–2011), Expert Opin. Ther. Patents 23 (2013) 319–331.

[35] S. Pardeep, R. Raghu, V. Kumar, M.P. Mahajan, P.M.S. Bedi, T. Kaur, A.K. Saxena, 1,2,3-Triazole tethered b-lactam-chalcone bifunctional hybrids: synthesis and anticancer evaluation, Eur. J. Med. Chem. 47 (2012) 594–600.
[36] E.N. da Silva Júnior, M.A.B.F. de Moura, A.V. Pinto, M.C.F.R. Pinto, M.C.B.V. de Souza, A.J. Araújo, C. Pessoa, L.V. Costa-Lotufo, R.C. Montenegro, M.O. de Moraes, V.F. Ferreira, M.O.F. Goulart, Cytotoxic, trypanocidal activities and physicochemical parameters of nor-beta-lapachone-based 1,2,3-triazoles, J. Braz. Chem. Soc. 20 (2009) 635–643.
[37] C.M. Zwaan, G.J. Kaspers, R. Pieters, W.N.L. Ramakers-Van, M.L. den Boer, R. Wünsche, M.M. Rottier, K. Hählen, E.R. van Wering, G.E. Janka-Schaub, U. Creutzig, A.J. Veerman, Cellular drug resistance profiles in childhood acute myeloid leukemia: differences between FAB types and comparison with acute lymphoblastic leucemia, Blood 96 (2000) 2879–2886.
[38] C.M. Zwaan, G.J. Kaspers, R. Pieters, K. Hählen, G.E. Janka-Schaub, C.H. van Zantwijk, D.R. Huismans, E. de Vries, M.G. Rots, G.J. Peters, G. Jansen, U. Creutzig, A.J. Veerman, Different drug sensitivity profiles of acute myeloid and lymphoblastic leukemia and normal peripheral blood mononuclear cells in children with and without Down syndrome, Blood 99 (2002) 245–251.
[39] C. Patel, L. Stenke, S. Varma, M.L. Lindberg, M. Björkholm, J. Sjöberg, K. Viktorsson, R. Lewensohn, O. Landgren, M.M. Gottesman, J.P. Gillet, Multidrug resistance in relapsed acute myeloid leukemia: evidence of biological heterogeneity, Cancer 119 (2013) 3076–3083.
[40] S.B. Ferreira, A.C. Sodero, M.F. Cardoso, E.S. Lima, C.R. Kaiser, F.P. Silva, V.F. Ferreira, Synthesis, biological activity, and molecular modeling studies of 1 H -1,2,3-triazole derivatives of carbohydrates as α-glucosidases inhibitors, J. Med. Chem. 53 (2010) 2364–2375.
[41] D.T.G. Gonzaga, M.R. Senger, F.C. da Silva, V.F. Ferreira, F.P. da Silva Jr., 1-Phenyl-1*H*- and 2-phenyl-2*H*-1,2,3-triazol derivatives: design, synthesis and inhibitory effect on alpha-glycosidases, Eur. J. Med. Chem. 74 (2014) 461–476.
[42] M.R. Senger, L.C. Gomes, S.B. Ferreira, C.R. Kaiser, V.F. Ferreira, F.P. da Silva Jr., Kinetics studies on the inhibition mechanism of pancreatic α-amylase by glycoconjugated 1*H*-1,2,3-triazoles: a new class of inhibitors with hypoglycemiant activity, ChemBioChem 13 (2012) 1584–1593.
[43] R. Abu Khalaf, A.M. Abdula, M.S. Mubarak, M.O. Taha, Discovery of new β-D-glucosidase inhibitors via pharmacophore modeling and QSAR analysis followed by in silico screening, J. Mol. Model. 17 (2011) 443–464.
[44] T.M. Gloster, P. Meloncelli, R.V. Stick, D. Zechel, A. Vasella, G.J. Davies, Glycosidase inhibition: an assessment of the binding of 18 putative transition-state mimics, J. Am. Chem. Soc. 129 (2007) 2345–2354.
[45] V.H. Lillelund, H.H. Jensen, X. Liang, M. Bols, Recent developments of transition-state analogue glycosidase inhibitors of non-natural product origin, Chem. Rev. 102 (2002) 515–553.
[46] S.D. Markad, N.S. Karanjule, T. Sharma, S.G. Sabharwal, D.D. Dhavale, Synthesis and evaluation of glycosidase inhibitory activity of N-butyl 1-deoxy-D-gluco-homonojirimycin and N-butyl 1-deoxy-Lido-homonojirimycin, Bioorg. Med. Chem. 14 (2006) 5535–5539.
[47] Y.L. Merrer, L. Gauzy, C. Gravier-Pelletier, J.C. Depezay, Synthesis of C2-symmetric guanidino-sugars as potent inhibitors of glycosidases, Bioorg. Med. Chem. 8 (2000) 307–320.
[48] I. Robina, P. Vogel, Synthesis of aza-C-disaccharides (dideoxyimino-alditols C-linked to monosaccharides) and analogues, Synthesis (2005) 675–702.
[49] J.W. Dennis, M. Granovsky, C.E. Warren, Glycoprotein glycosylation and cancer progression, Biochim. Biophys. Acta 1473 (1999) 21–34.
[50] S. Gerber-Lemaire, L. Juillerat-Jeanneret, Glycosylation pathways as drug targets for cancer: glycosidase inhibitors, Mini Rev. Med. Chem. 6 (2006) 1043–1052.
[51] D. Gupta, K. Podar, Y. Tai, B. Lin, T. Hideshima, M. Akiyama, R. LeBlanc, L. Catley, N. Mitsiades, C. Mitsiades, D. Chauhan, N.C. Munshi, K.C. Anderson, Beta-lapachone, a novel plant product, overcomes drug resistance in human multiple myeloma cells, Exp. Hematol. 30 (2002) 711–720.
[52] D.E. Clark, S.D. Pickett, Computational methods for the prediction of drug likeness, Drug Discov. Today 5 (2000) 49–58.
[53] J.E. Kim, H.J. Cho, J.S. Kim, C.K. Shim, S.J. Chung, M.H. Oak, I.S. Yoon, D.D. Kim, The limited intestinal absorption via paracellular pathway is responsible for the low oral bioavailability of doxorubicin, Xenobiotica 43 (2013) 579–591.
[54] S. Jain, S.R. Patil, N.K. Swarnakar, A.K. Agrawal, Oral delivery of doxorubicin using novel polyelectrolyte-stabilized liposomes (layersomes), Mol. Pharm. 9 (2012) 2626–2635.
[55] M.I. Gharib, A.K. Burnett, Chemotherapy-induced cardiotoxicity: current practice and prospects of prophylaxis, Eur. J. Heart Fail. 4 (2002) 235–242.
[56] Y. Shi, M. Moon, S. Dawood, B. McManus, P.P. Liu, Mechanisms and management of doxorubicin cardiotoxicity, Herz 36 (2011) 296–305.
[57] Z. Wang, Y. Chen, H. Liang, A. Bender, R.C. Glen, A. Yan, P-glycoprotein substrate models using support vector machines based on a comprehensive data set, J. Chem. Inf. Model. 51 (2011) 1447–1456.
[58] C. Obiol-Pardo, J. Gomis-Tena, F. Sanz, J. Saiz, M. Pastor, A multiscale simulation system for the prediction of drug-induced cardiotoxicity, J. Chem. Inf. Model. 51 (2011) 483–492.
[59] R. Huisgen, G. Szeimies, L. Moebius, 1.3-Dipolare cycloadditionen, XXXII. Kinetik der Additionen organischer Azide an CC-Mehrfachbindungen, Chem. Ber. 100 (1967) 2494–2507.
[60] H.C. Kolb, M.G. Finn, K.B. Sharpless, Click chemistry: diverse chemical function from a few good reactions, Angew. Chem. Int. Ed. 40 (2001) 2004–2021.
[61] S.B. Ferreira, F.C. da Silva, A.C. Pinto, D.T.G. Gonzaga, V.F. Ferreira, Syntheses of chromenes and chromanes via o-quinone methide intermediates, J. Heterocycl. Chem. 46 (2009) 1080.
[62] F.C. da Silva, S.B. Ferreira, C.R. Kaiser, A.C. Pinto, V.F. Ferreira, Synthesis of a- and b-lapachone derivatives from hetero diels-alder trapping of alkyl and aryl o-quinone methides, J. Braz. Chem. Soc. 20 (2009) 1478–1482.
[63] S.B. Ferreira, D.R. da Rocha, J.W.M. Carneiro, W.C. Santos, V.F. Ferreira, A new method to prepare 3-alkyl-2-hydroxy-1,4-naphthoquinones. Synthesis of lapachol and phthiocol, Synlett (2011) 1551–1554.
[64] T. Sander, J. Freyss, M. von Korff, J.R. Reich, C. Rufener, OSIRIS, an entirely in-house developed drug discovery informatics system, J. Chem. Inf. Model. 49 (2009) 232–246.
[65] C.A. Lipinski, F. Lombardo, B.W. Dominy, P.J. Feeney, Experimental and computational approaches to estimate solubility and permeability in drug discovery and development settings, Adv. Drug Deliv. Rev. 46 (1997) 3–26.
[66] C. Feixiong, W. Li, Y. Zhou, J. Shen, Z. Wu, G. Liu, P.W. Lee, Y. Tang, admetSAR: a comprehensive source and free tool for evaluating chemical ADMET properties, J. Chem. Inf. Model. 52 (2012) 3099–3105.